Applied Water Science (2021) 11:1
https://doi.org/10.1007/s13201-020-01330-z

ORIGINAL ARTICLE

Evaluation of alkaline-based activated carbon from *Leucaena Leucocephala* produced at different activation temperatures for cadmium adsorption

Wan Muhammad Hilmi Wan Ibrahim[1] · Mohd Hazim Mohamad Amini[1] · Nurul Syuhada Sulaiman[2] · Wan Rasidah Wan Abdul Kadir[3]

Received: 7 July 2020 / Accepted: 16 November 2020 / Published online: 1 December 2020

Abstract

Heavy metal contamination in water is happening worldwide. Adsorption using activated carbon is a common choice for cleaning the wastewater. The drawback of activated carbon is the higher cost of production due to the need for high heat in the process. This work investigated on activated carbon produced from the abundantly available *Leucaena leucocephala* biomass in order to reduce the cost of raw material. The biomass was chemically activated at different activation temperatures. The produced activated carbon was characterized using SEM, FT-IR, surface analyzer, and TGA. Isothermic and thermodynamic studies were done to evaluate the adsorption properties of the activated carbon. It was found out that higher surface area can be obtained using the higher activation temperature. Higher NaOH to carbonized sample ratios also resulted in higher surface area for all activation temperatures, which are 662 m^2g^{-1} for 700 °C activation temperature, 735 m^2g^{-1} for 750 °C, and 776 m^2g^{-1} for 800 °C. Isothermic studies showed that all of the activated carbon that is produced from *Leucaena leucocephala* biomass are fit to the Langmuir isotherm, regardless of any activation temperature. Lastly, the thermodynamic study found out the adsorption process is endothermic, reflected by the positive value of ΔH^o. It can be concluded that *Leucaena leucocephala* is a promising alternative material for producing activated carbon.

Keywords Activated carbon · *Leucaena leucocephala* · Cadmium · Adsorption · Isothermic · Thermodynamic

Introduction

Heavy metals have been associated with toxic elements. They have been listed in the United States Environmental Protection Agency (USEPA) as a pollutant that needs to be controlled and addressed (Gupta et al. 2002). Any form of metal, mineral salts, and trace elements has a specific function. Some need each other to work optimally. However, some substances will cause harm to the body at a specific threshold with toxic side effects (Rafatullah et al. 2011). It is even more unfortunate if the presence of the material cannot be accurately confirmed until symptoms arise. The materials or metals often associated with such phenomena are lead, cadmium, and chromium (Singh et al. 2007).

In developing countries, various types of development projects are being implemented and involve varying degrees of environmental disturbance. Because of these developments, various problems have cropped up in the course of these developments. The most significant effect is the impact on human health. When humans are exposed to heavy metals for an extended period, it can cause serious health problems such as cancer (Lee et al. 2018).

Cadmium is one of the dangerous heavy metals utilized by humans for various material industries. It is used in battery manufacturing. It is beneficial, but it could be a danger to human health when it exposes to water (Wu et al. 2016). In industrial settings, cadmium waste flowed into the water and resulted in hazardous exposure to human health. Cadmium is present as a by-product of the filtration of some heavy metals such as lead and zinc. The danger of cadmium

✉ Mohd Hazim Mohamad Amini
hazimamini@gmail.com

[1] Faculty of Bio-Engineering and Technology, Universiti Malaysia Kelantan, 17600 Jeli, Kelantan, Malaysia

[2] School of Industrial Technology, Universiti Sains Malaysia, 18000 George, Penang, Malaysia

[3] Forest Research Institute Malaysia, 52109 Kepong, Kuala Lumpur, Selangor, Malaysia

is that it can enter our bodies through food, and for long-term exposure, it could lead to serious health problems like cancer (Chunhabundit 2016).

The case of cadmium poisoning happened in a few countries around the world. Japan experienced cadmium poisoning in 1974. The pollution is caused by the disposal of lead–zinc mining waste, which contains cadmium into the Jintsu River. Overflowing of polluted rivers flooded the rice fields, which resulted in the absorption of cadmium into rice plants. This has an impact on the content of cadmium in rice, whereby it reaches between 3 and 4 µg cadmium per kg (Uetani et al. 2006).

Various water treatment techniques were applied, including the adsorption, reverse osmosis membrane, solvent extraction, and high technology ultrafiltration process (Li et al. 2020a). The adsorption method is being the most popular due to lower operation costs and simple implementation (Li et al. 2019b). The activated carbon is a popular choice of material for water treatment. Activated carbon is solid charcoal that has been further processed so that it has better properties as an adsorbent. The ability of activated carbon as an adsorbent is caused by the formation of pores on the charcoal due to the carbonization and activation process (Bansal and Goyal 2005). Properties of activated carbon are affected by the type of raw material and its manufacturing conditions (Ningrum et al. 2008). Due to several factors such as renewability, lower cost, and environmentally friendly, biomass-derived activated carbons are chosen by many industrial players (Li et al. 2018). Raw materials that can be used as activated carbon are all carbonaceous, whether derived from plants, animals, or minerals. The materials are various types of wood, rice husks, animal bones, coal, coconut shell, coffee bean skin, and so forth (Subadra et al. 2005).

The primary function of activated carbon in the industry is as a hazardous material adsorbent (Kurniawan 2004). In addition to adsorbents, activated carbon can be used as decolorizer, deodorizer, water purification, and waste treatment (Smíšek and Černý 1970). The advantage of using activated carbon in wastewater processing is that the activated carbon can reduce water contaminants in a large and absorptive capacity. The disadvantage of activated carbon is the price, which is quite expensive and may not be under the purchasing power of the community, resulting in people using non-active carbon. Non-active carbon is carbon that does not undergo the activation process (Alimsyah and Damayanti 2013). However, activated carbon production is still the primary choice as it requires less technological advances compared to the production of the superadsorptive carbon nanotubes while still maintaining high efficiency in hazardous material removal from wastewater (Li et al. 2020b).

There are three activation methods of preparing activated carbon, namely physical activation, chemical activation, and physiochemical activation (Sulaiman et al. 2018). In this work, activated carbon was produced through the chemical activation method. The chemical activation by alkalis involves solid–solid or solid–liquid reactions, besides the hydroxide reduction and carbon oxidation to generate porous structures in the carbonized material (Adinata et al. 2007). This method involves precursor carbonization in the presence of alkali hydroxides, within a single- or two-step process. The KOH, NaOH, K_2CO_3, $ZnCl_2$, $FeCl_3$, H_3PO_4, and H_2SO_4 are among the reagents used, and the activation process needs a lower temperature than the physical activation (Yang and Qiu 2010).

The carbonization or pyrolysis of the raw material was initially done by heating at temperatures between 300 °C and 500 °C to form the char or carbonized material (Wong et al. 2018). The carbonized sample as the precursor was mixed or soaked in alkaline reagent at pre-determined ratio before dried. Dried mixtures were heated at temperature closed above 400 °C in a closed or inert gas-filled atmosphere for specific period to complete the activation process. The examples of raw materials, with their activating chemicals and activating temperatures, are shown in Table 1. The surface area of the resulting activated carbon varies between 770 and 3300 m^2g^{-1}.

In the physical activation method, the formation of pores is mainly due to the removal of carbon atoms by gasification. In contrast, the chemical activation works with dehydrogenation of the precursor by the activating agents to form cross-links between carbons, which later creates the pores on the surface of activated carbon (Liu et al. 2010). Compared to the physical activation, the chemical activation method will usually produce a higher yield (Shi et al. 2010). The chemical activation can also be conducted at a lower temperature compared to physical activation, which reduces energy usage. Other advantages of chemical activation are lesser activation time, the possibility to incorporate suitable functional groups, and production of larger surface area, which are essential for the adsorption process. However, chemical activation requires activating reagents which increase the production price (Danish and Ahmad 2018).

In this work, the *Leucaena leucocephala* biomass was chemically activated at different activation temperatures. *Leucaena leucocephala* is also locally known as Petai Belalang, a tree that is originated from Central America. The Portuguese and the Dutch brought the species to Asian parts in the seventeenth century (Hou et al. 2015). It is a very fast-growing tree which reaches a height of more than 6 m in only two to three years, yielding high biomass productivity at more than 50 ton ha^{-1} annually (Loaiza et al. 2017). The *Leucaena leucocephala* can be easily cultivated, with most of them wildly grown by themselves. Currently, this tree was only used for animal feed and for burning, which showed lower value usage of the biomass. There are lacks of

Table 1 Activated carbon produced by chemical activation

Precursor	Activating agent	Activation temperature (°C)	Surface area (m^2g^{-1})	References
Coffee bean husk	H_3PO_4	450	1402	(Kim et al. 2005)
Bamboo	H_3PO_4	600	1432	(Wang et al. 2006)
Golden shower	K_2CO_3	800	1413	(Tran et al. 2017)
Bituminous coal	$ZnCl_2$	600	960	(Meng et al. 2005)
Bituminous coal	KOH	800	3300	(Meng et al. 2005)
Coconut shells	$ZnCl_2$	560 W (Microwave radiation)	794.84	(Li and Jaroniec 2001)
Olive-mill wastewater	KOH	800	1768	(Lee et al. 2006)
Cotton stalks	H_3PO_4	420	834	(Kim et al. 2004)
Petroleum coke	KOH	800	1798	(Ryoo et al. 2001)
Antibiotic waste	K_2CO_3	900	1170	(Gierszal et al. 2006)
Chestnut wood	H_3PO_4	500	783	(Yang et al. 2004)

research done on *Leucaena leucocephala* as activated carbon to date. The abundant availability of *Leucaena leucocephala* could be an advantage as a cheap and continuously available raw material for activated carbon production. Later in this work, the produced activated carbons were subjected to characterization and tested for cadmium adsorption. Langmuir and Freundlich isotherms which were commonly used to study the behavior of adsorption were also applied in this work (Li et al. 2019a).

Experimental

Raw material preparation

Wild *Leucaena leucocephala* biomass was collected around Selangor, Malaysia. The sample was left to air dry to prevent difficulties in the size reduction process to a moisture content of below 10%. Chipped samples were then grounded and sieved into particle size between 1 and 2 µm. Final moisture content was determined using the oven-dry method before kept in an air-tight container for further use (Rafatullah et al. 2011).

Conversion into activated carbon

Carbonization was done by batch using a pyrolyzer with approximately 6 kg of raw *Leucaena leucocephala* biomass for each batch. The activation process was conducted by chemical means. Sodium hydroxide, NaOH, and carbonized *Leucaena leucocephala* biomass were mixed using impregnation ratio NaOH: char of 3:1, 2:1 and 1:1. Approximately 10 g of carbonized *Leucaena leucocephala* was homogenized with a pre-determined amount of NaOH in 100 mL distilled water. Continuous stirring was done for two h before heated in an oven at 105 °C for 24 h (Cazetta et al. 2011). After 24 h, NaOH-impregnated char was activated inside a muffle furnace using temperatures of 700 °C, 750 °C, and 800 °C for 90 min. Continuous nitrogen gas flow of 150 cm^3/min into the furnace was ensured until samples were cooled down to prevent oxidation. All of the prepared samples are tabulated in Table 2.

Adsorbent characterization

Raw and activated carbon samples of *Leucaena leucocephala* were sprinkled on separate aluminum stub stickled with glue before analysis. Samples were observed using scanning electromagnetic imaging, SEM (JSM-IT100 JEOL Co.), at suitable magnifications. The surface area of activated carbon produced was determined using a Micromeritics (ASAP 2010) gas adsorption surface analyzer through nitrogen adsorption isotherm at 77°K. Calculation of surface area was done based on Brunauer–Emmett–Teller equation (BET). Surface functional

Table 2 Prepared activated carbon samples

No.	Sample code	Temperature	NaOH: char ratio
1	C3-700	700	3:1
2	C2-700	700	2:1
3	C1-700	700	1:1
4	C3-750	750	3:1
5	C2-750	750	2:1
6	C1-750	750	1:1
7	C3-800	800	3:1
8	C2-800	800	2:1
9	C1-800	800	1:1

groups of the samples were analyzed using Thermo Scientific Nicolet iS10 FTIR Spectrometer. Samples were grounded into a fine powder before scanned between 4000 and 400 cm^{-1}. Thermogravimetric analysis was done using Mettler Toledo Thermogravimetric Analyzer TGA/DSC 1. The sample was heated at a rate of 10 °C/min with a temperature sweep between 30 °C and 900 °C.

Isothermic studies

A stock solution of cadmium of 1000 ppm was prepared from cadmium nitrate powder. Stock solution was diluted into different concentrations of 10, 15, 20, 25, 30, 33, 35, 40, 45, and 50 ppm. Approximately 50 ml of adsorbate was mixed with 0.5 g activated carbon in different conical flasks. Conical flasks were shacked for 160 min, as previously determined in the batch adsorption study on the effect contact time (Wan Ibrahim et al. 2019). Three temperatures were used, including 30 °C, 40 °C, and 50 °C. Mixtures were filtered with filter paper, and filtered solutions were analyzed using inductively coupled plasma optical emission spectrometry (ICP-OES).

Langmuir and Freundlich's model had been applied to evaluate the adsorption behavior of the adsorbate onto the adsorbent. Langmuir isotherm model suggested ideal monolayer adsorption onto a homogenous surface, calculated using Eq. 1:

$$\frac{1}{q_e} = \frac{1}{q_m} + \frac{1}{K_a q_m C_e} \tag{1}$$

where q_e is the amount of adsorbate adsorbed at equilibrium per gram of sample (mg/g), q_m is the saturated amount of adsorbate adsorbed in mg/g, C_e is the equilibrium concentration of cadmium in mg/l, and Ka is the Langmuir adsorption constant in l/mg. A slope of $1/K_a q_m$ was obtained from $1/q_e$ versus $1/C_e$ plot with an intercept at $1/q_m$.

The Freundlich isotherm assumes heterogeneous, and multilayer adsorption occurred on the adsorbent surface (Çetinkaya et al., 2018), calculated using Eq. 2:

$$\ln q_e = \ln K_F + \frac{1}{n} \ln C_e \tag{2}$$

where K_F is Freundlich equilibrium constant, n is an empirical constant and others, as stated in Eq. 1. A slope of (1/n) was derived from a plot of ln qe vs. ln C_e with an intercept of $\ln K_F$.

Results and discussion

Surface morphology analysis

Figure 1 shows the 150x and 550x magnified SEM images of the raw *Leucaena leucocephala,* carbonized sample, and the activated carbon. Some minor pores were observed on the raw material's surface, while the carbonization process creates more holes and cavities. The carbonized samples possessed very little tiny holes or pores because of the incomplete decomposition of organic constituents that exist in the carbonaceous precursors. The pores were typically blocked by the carbonization product residue (Rahman and Saad 2003). Pores available on the surfaces of the activated carbons prepared from *Leucaena leucocephala* were well pronounced with distinct pore walls. They were arranged in a group of honeycombed structures. The carbonization product residue, which blocked the pores on the char, was gasified by the activation process. They were carried away with the exhaust gas leaving most of the pores clear and easily absorbable by the cations. At 2000x magnification, the metals can be seen agglomerated inside the pore of the adsorbent (Fig. 2). Because of well-developed porosities formed by the sodium hydroxide, the adsorption capacity of activated carbon and the surface area on the *Leucaena leucocephala* has increased.

Surface area

BET surface area of prepared activated carbon is shown in Table 3. Using an activation temperature of 800 °C resulted in a higher surface area, which is 185 m^2g^{-1} for ratio 1:1, 595 m^2g^{-1} for ratio 2:1, and 776 m^2g^{-1} for ratio 3:1. The higher surface area was formed using the highest activation temperature. Higher NaOH to carbonized sample ratios also resulted in higher surface area for all activation temperatures, which are 662 m^2g^{-1} for 700 °C activation temperature, 735 m^2g^{-1} for 750 °C, and 776 m^2g^{-1} for 800 °C. This trend was similarly recorded from the previous study by Cazetta et al. (2011), which also used NaOH as the activating agent.

Fourier transform spectroscopy, FT-IR analysis

FT-IR analysis provides information about the molecular structure of the functional groups present on the samples under investigation. Figure 3 shows the infrared spectra of all samples. The raw *Leucaena leucocephala* biomass showed a higher number of peaks. The C–H group was detected at 2895.87 cm^{-1} and 826.79 cm^{-1}. The C–N groups were detected at the wave number of 2112.37 cm^{-1} and 1027.53 cm^{-1}. Imines group was detected at the wave number of 3332.59 cm^{-1}, while the urethanes group was detected at the wave number of 1731.58 cm^{-1}. The infrared spectra of activated carbon with an activation temperature of 700 °C, 750 °C, and 800 °C showed alkyne group at the wave number of 2108.77 cm^{-1}. The O–H group was detected at the wave number of 1400.35 cm^{-1}, and the hydrocarbon group was detected at the wave number of 872.29 cm^{-1}. Details of infrared spectra interpretation for

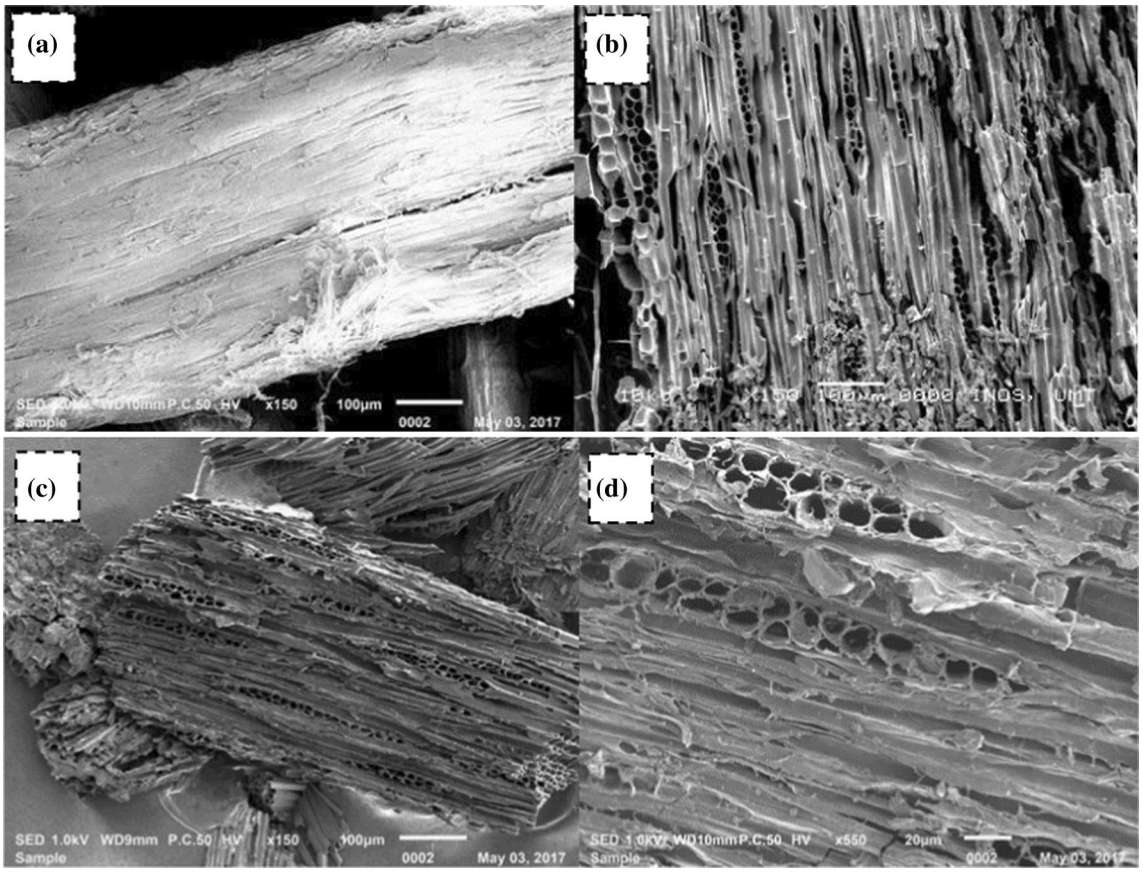

Fig. 1 SEM images of *Leucaena leucocephala* before carbonization **a**, after carbonization **b**, and after activation **c** at magnification 150x as well as activated carbon at magnification 550x **d**

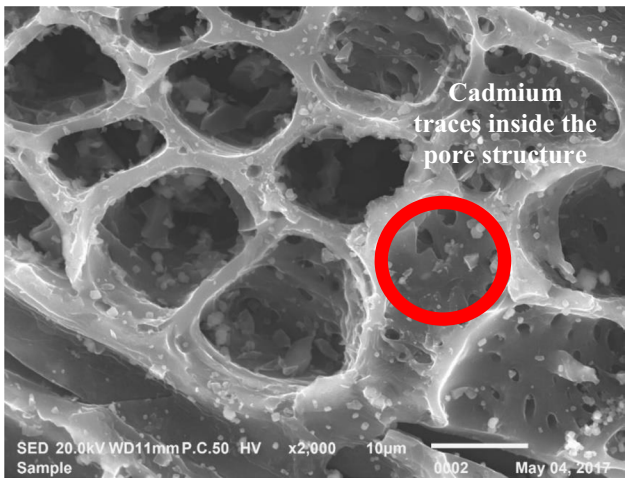

Fig. 2 SEM image of activated carbon after the adsorption process at magnification 2000x

Table 3 BET surface area of prepared activated carbon

No.	Sample code	BET Surface area (m^2/g^{-1})
1	C1-700	120
2	C2-700	483
3	C3-700	662
4	C1-750	140
5	C2-750	531
6	C3-750	735
7	C1-800	185
8	C2-800	595
9	C3-800	776

activated carbon are shown in Table 4. There was a lesser number of functional groups found in the activated carbon compared to raw *Leucaena leucocephala*. During the activation stage, the chemical-activating agent broke many bonds comprise aliphatic and aromatic species in the lignocellulosic precursor (Gerçel et al. 2007).

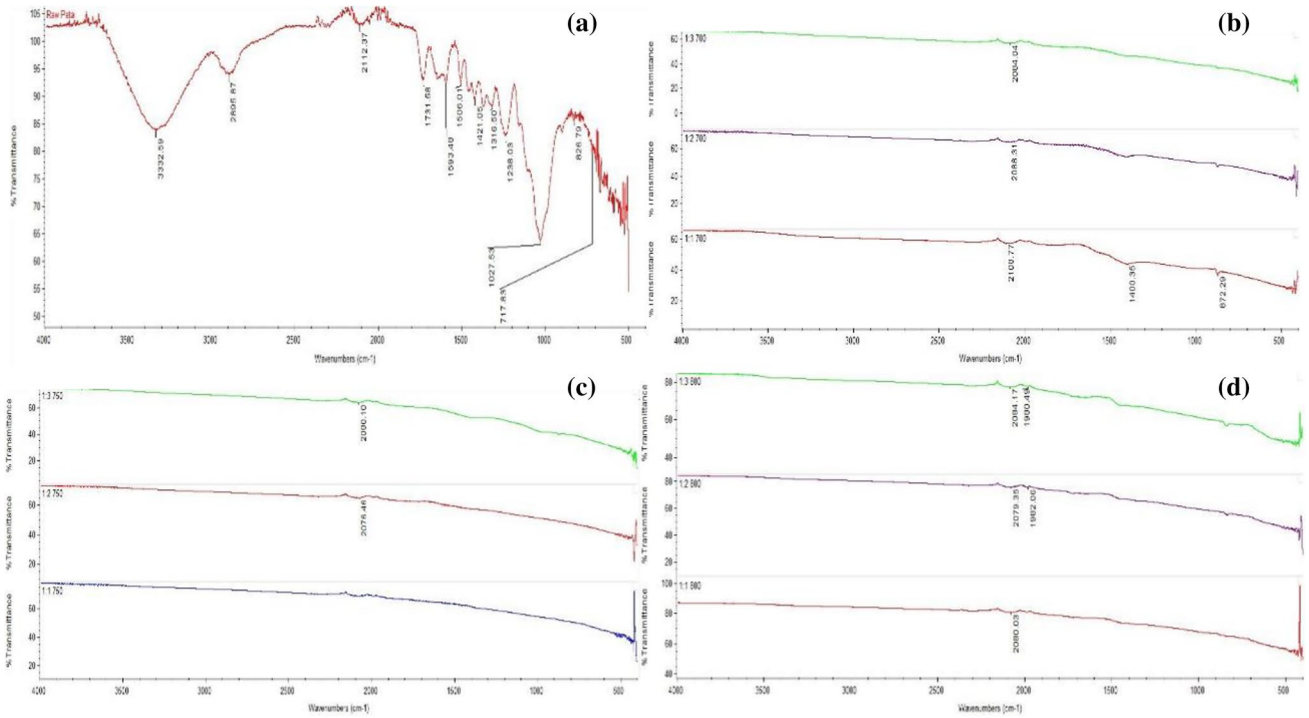

Fig. 3 FT-IR spectra for raw *Leucaena leucocephala* biomass **a**, samples with activation temperature 700 °C, **b** 750 °C, and **c** 800 °C **d**

Table 4 Detail interpretation of FT-IR spectra

Activation temperature, °C	Peak, cm^{-1}	Assigned group	Details
Raw sample	**3332.59**	Imines	(=N—N); one band, Amine salts
	2895.87	Alkane	C—H stretching, hydrocarbon chromophore
	2112.37	Isocyanides	C—N stretching, Unsaturated nitrogen compounds
	1731.58	Urethanes	Carbonyl stretching, Amides
	1593.48	Primary	N—H stretching, Amines
	1506.01	Aromatic	C—NO_2 nitro compounds, Unsaturated nitrogen compounds
	1421.05	Sulfites	S = O stretching, Sulfur compounds
	1316.50	Sulfonamides	S = O stretching, Sulfur compounds
	1238.03	Nitrates	O–NO_2, Unsaturated nitrogen compounds
	1027.53	Aliphatic	C—N vibrations, Amines
	826.79	Alkene, trisubstituted	C—H bending, Hydrocarbon chromophore
700	**2108.77**	Alkyne, monosubstituted	C—C multiple bond stretching
	2084.04	Isocyanides	C—N stretching vibrations, Unsaturated nitrogen compounds
	1400.35	Miscellaneous chromophoric groups	O—H bending and C–O, Phenols
	872.29	Hydrocarbon chromophore	C—H bending, One hydrogen atom
750	**2080.10**	Isocyanides	C—N stretching vibrations, Unsaturated nitrogen compounds
	2080.03	Isocyanides	C—N stretching vibrations Unsaturated nitrogen compounds
	1980.49	Allene	C—C multiple bond stretching
800	**2084.17**	Isocyanides	C—N stretching vibrations Unsaturated nitrogen compounds
	2080.03	Isocyanides	C—N stretching vibrations Unsaturated nitrogen compounds
	2079.35	Isocyanides	C—N stretching vibrations Unsaturated nitrogen compounds
	1980.49	Allene	C—C multiple bond stretching

Thermal gravimetry analysis, TGA

Generally, there are three stages for thermal gravimetry curves, comprising of the first stage as loss of moisture in the adsorbent, second stage 2 for degassing, and final stage is the residue of the adsorbent. Figure 4 shows the thermal gravimetry curves for activated carbon from *Leucaena leucocephala* biomass. All of the samples showed an initial decrement of weight at about 10%, which was due to loss in moisture and volatiles. Stage 2 of weight reduction between 200 °C and 500 °C corresponds to the degradation of the polymeric material such as cellulose (Amini et al. 2019). All activated carbon products showed significantly less weight loss compared to the raw biomass, as the lignocellulosic components mostly had been degraded through the pyrolyzing and activation process. Even though the activated carbon made using higher NaOH: biomass ratio has the highest surface area, they are a little less thermally stable compared to the lower ratios at all activation temperatures. For the activation temperature 700 °C, the residue for the ratio 1:1 (C1-700) is 80.58%, for 2:1 (C2-700) is 79.41%, and for the ratio 3:1 (C3-700) is 78.66%. The same goes for the activation temperature of 750 °C and 800 °C. Higher activation temperature also reduces the thermal stability of the activated carbon. Sample from the activation temperature 700 °C resulted in higher residual content, which is 80.58%, while the 750 °C activation temperature results in the residual content of 80.46%. The 800 °C activation temperature resulted in lower 74.93% in the residue. This result was similarly reported from the previous study by Le Van and Luong Thi (2014), which showed increasingactivation temperature resulted in lower residual content.

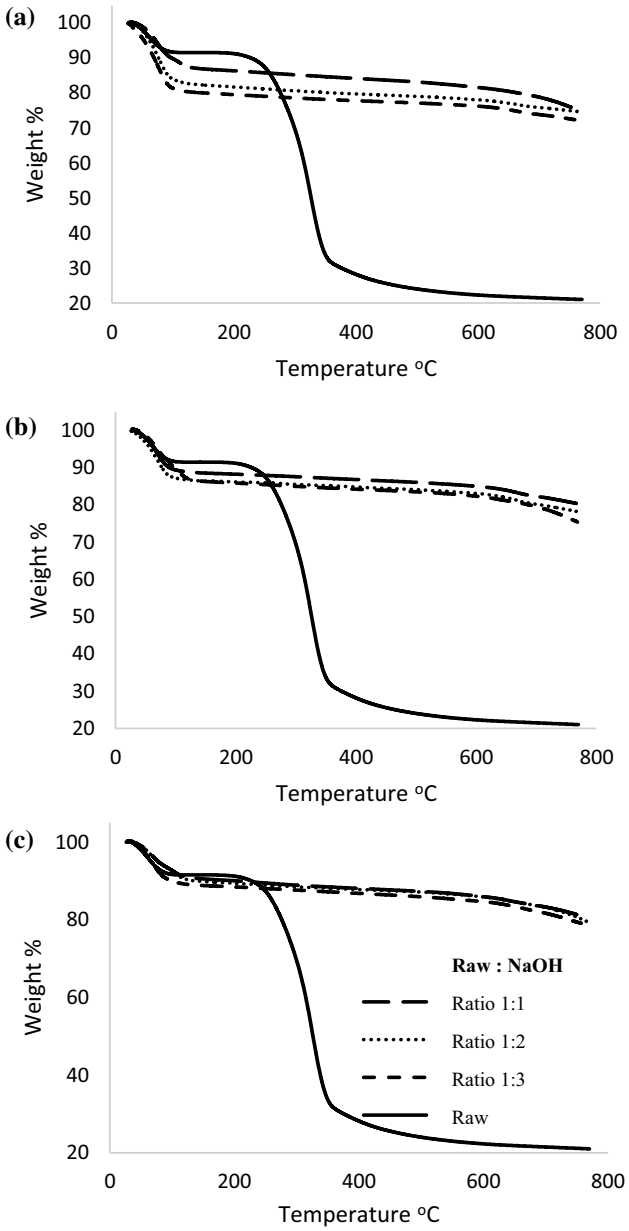

Fig. 4 Thermal gravimetry curve for samples produced at 700 °C (**a**), 750 °C (**b**), and 800 °C (**c**) activation temperatures

Isothermic studies

Langmuir isotherm

Figure 5 shows Langmuir isotherm plots of 1/Qe versus 1/Ce for all samples at 30 °C, 40 °C, and 50 °C. The R^2 values for the C1-700 were 0.9925, 0.9506, and 0.9728 at 30 °C, 40 °C, and 50 °C, respectively. The constant q_m, which is a measure of the adsorption capacity to form a monolayer, was found to be as high as 196.078 mg/g at 50 °C. Constant K_L, which denotes adsorption energy, for the corresponding adsorption capacity is between 0.227 and 2.029 l/mg. For C2-700, the R^2 values are 0.9933, 0.9879, and 0.9686 at 30 °C, 40 °C, and 50 °C, respectively. The highest value for constant q_m, which is a measure of the adsorption capacity to form a monolayer, was 95.238 mg/g at 30 °C. Constant K_L, which denotes adsorption energy, for the corresponding adsorption capacity is between 1.280 and 4.440 l/mg. C3-700 resulted in a correlation coefficient of 0.9700, 0.9325, and 0.9776 at 30 °C, 40 °C, and 50 °C, respectively. The highest constant q_m was 67.114 mg/g at 30 °C. Constant K_L was between 1.317 and 3.667 l/mg.

The value of the correlation coefficient for C1-750 was 0.9702, 0.9804, and 0.9588 at 30 °C, 40 °C, and 50 °C, respectively. The highest q_m was 89.256 mg/g at 50 °C. Constant K_L is between 0.684 and 1.261 l/mg. C2-750 showed the value of correlation coefficient of 0.9850, 0.9813, and 0.9752 at 30 °C, 40 °C, and 50 ℃, respectively. The highest constant q_m is 46.729 mg/g at 50 °C, and the constant K_L was between 3.262 and 9.804 l/mg. C3-750 showed a correlation coefficient of 0.9884, 0.9774,

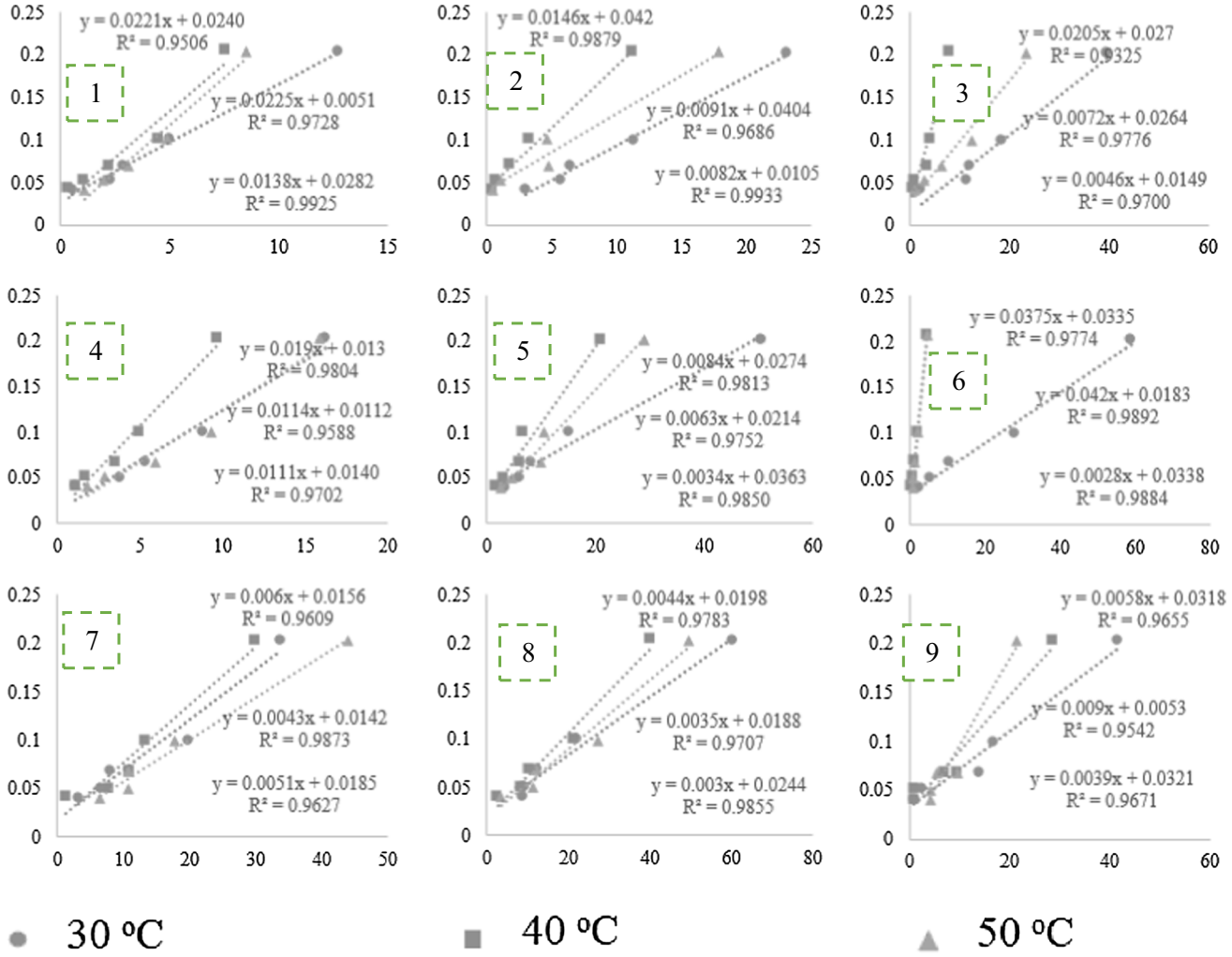

Fig. 5 Langmuir plot of 1/Qe vs 1/Ce for samples C1-700 (1), C2-700 (2), C3-700 (3), C1-750 (4), C2-750 (5), C3-750 (6), C1-800 (7), C2-800 (8), and C3-800 (9) at 30 ℃, 40 ℃, and 50 ℃

and 0.9892 at 30 °C, 40 °C, and 50 ℃, respectively. The highest q_m was 54.645 mg/g at 50 °C, while the constant K_L was between 0.436 and 12.071 l/mg.

The R^2 values for C1-800 are 0.9627, 0.9609, and 0.9873 at 30 °C, 40 °C, and 50 °C, respectively. The maximum value of constant q_m was 70.423 mg/g at 50 °C, and the constant K_L was between 2.600 and 3.627 l/mg. The R^2 values for C2-800 are 0.9855, 0.9783, and 0.9707 at 30 °C, 40 °C, and 50 °C, respectively. The constant q_m, which is a measure of the adsorption capacity to form a monolayer, is reported to be as high as 53.191 mg/g at 50 °C. Constant K_L showed values between 4.500 and 8.133 l/mg. For C3-800, the R^2 values are 0.9671, 0.9655, and 0.9542 at 30 °C, 40 °C, and 50 °C, respectively. The constant q_m was 188.67 mg/g at 50 °C. Constant K_L was valued between 0.589 and 8.231 l/mg.

Freundlich isotherm

The plot of linearized equations for Freundlich for the adsorption of cadmium is shown in Fig. 6. The Freundlich model is applicable for non-ideal sorption on heterogeneous surfaces and multilayer sorption processes. The correlation coefficients for the adsorption of cadmium ions for C1-700 were 0.8700, 0.8662, and 0.9454 for 30 °C, 40 °C, and 50 °C, respectively. C2-700 showed 0.9672, 0.9893, and 0.8870, while C3-700 showed 0.7956, 0.8222, and 0.9082 for the correlation coefficient, 30 °C, 40 °C, and 50 °C, respectively.

The values of 1/n were obtained from the slope of the plotted graph ln qe versus ln Ce. The n value lying between 1 and 10 indicates a favorable condition for adsorption. The C1-700 sample showed 1/n values of 1.3812, 1.3320,

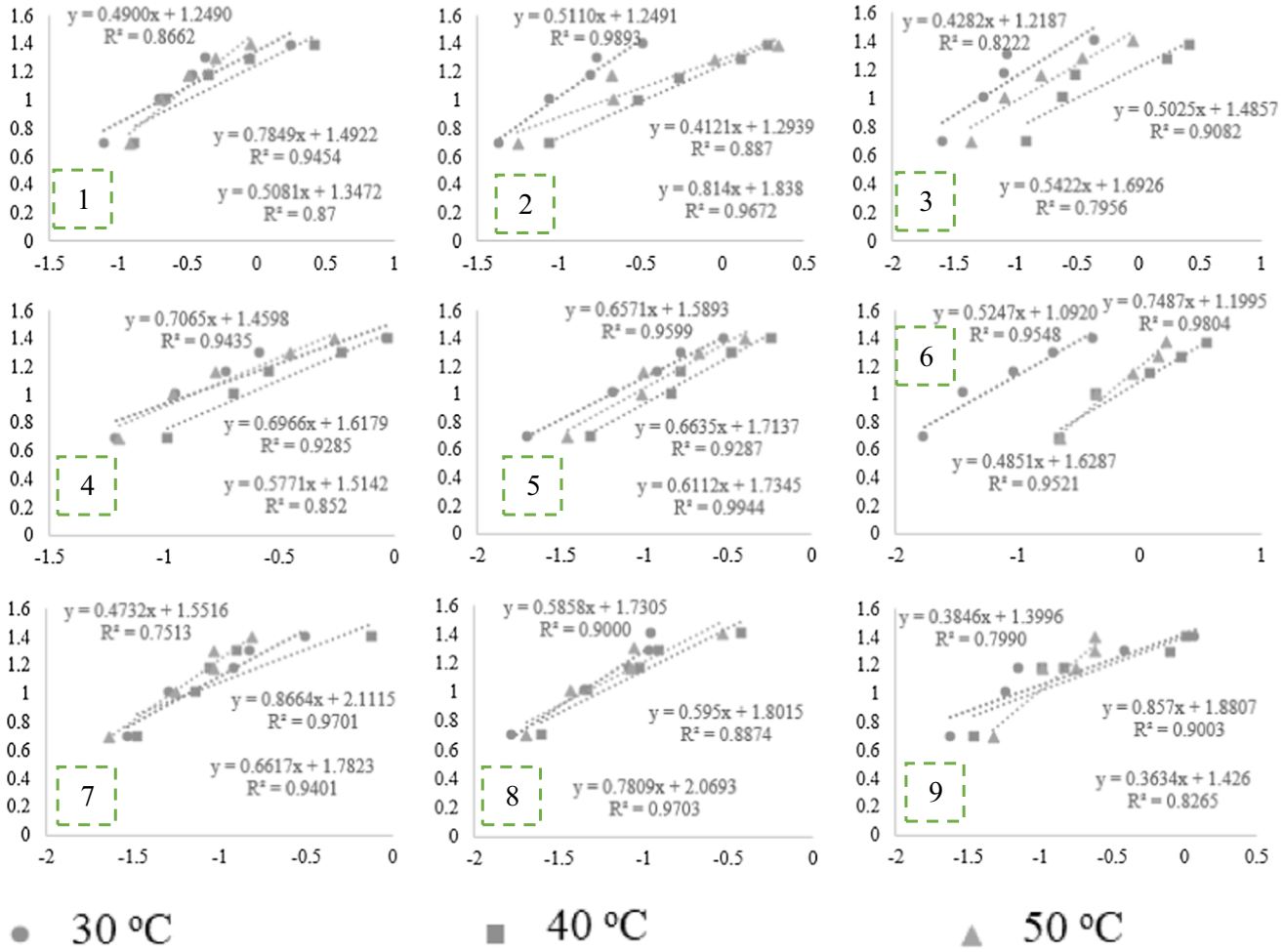

Fig. 6 Linear regression analysis of Freundlich isotherm for samples C1-700 (1), C2-700 (2), C3-700 (3), C1-750 (4), C2-750 (5), C3-750 (6), C1-800 (7), C2-800 (8), and C3-800 (9) at 30 ℃, 40 ℃, and 50 ℃

and 2.1336 for 30 °C, 40 °C, and 50 °C, respectively. The C2-700 showed 1/n values of 2.2217, 1.3890, and 1.1202 for 30 °C, 40 °C, and 50 °C, respectively, while C3-700 showed 1.4739, 1.1640, and 1.3659 for 30 °C, 40 °C, and 50 °C, respectively. The value of 1/n for C1-750 was 1.5144, 1.9205, and 1.8936 for 30 °C, 40 °C, and 50 °C, respectively. For C2-750, the values were 1.6614, 1.7862, and 1.8036 for 30 °C, 40 °C, and 50 °C, respectively, while C3-750 showed 1/n values of 1.3186, 1.4263, and 2.0352 for 30 °C, 40 °C, and 50 °C, respectively. For C1-800, the value of 1/n was 1.7987, 1.2863, and 2.3551 for 30 °C, 40 °C, and 50 °C, respectively. The C2-800 recorded 2.1227, 1.5924, and 1.6174 for 30 °C, 40 °C, and 50 °C, respectively, and C3-800 showed 0.9878, 1.0455, and 2.3296 for 30 °C, 40 °C, and °C, respectively. All of the samples showed favorable condition for adsorption except for C3-800 at 30 °C. However, the value is very closed to a favorable region at 0.9878.

Table 5 shows the different R^2 values for both isotherms, Langmuir and Freundlich, for the adsorption of cadmium. The R^2 value for samples with an activation temperature of 700 °C shows that the Langmuir model has a value of correlation coefficient close to 1 and more fit to the Langmuir isotherm instead of Freundlich. All of the activated carbon that is produced from *Leucaena leucocephala* biomass are fit to the Langmuir isotherm for all activation temperature. This concludes that the activated carbon produced is doing monolayer cadmium adsorption onto the surface (Sulaiman et al. 2010).

Thermodynamic analysis

The adsorption characteristic of cadmium ions onto chemical activated carbon made from *Leucaena leucocephala* biomass had been studied in the thermodynamic parameters. Three parameters were studied which were the ΔG^o as Gibb's free energy change, kJ/mole, ΔH^o as enthalpy change, J/mol, and ΔS^o as entropy change, J/K/mol. The linearized equation is as in Eqs. 3, 4;

$$G^o = -RT \ln\left(K_L\right) \tag{3}$$

$$G^o = H^o - TS^o \tag{4}$$

The R is 8.314 J/K/mol, which is universal gas constant, and T value is the temperature in the Kelvin scale. K_L was described as a value of Langmuir constant. Figure 7 presents the slopes of the linear lines, which were either positive or negative depending on the adsorbate–adsorbent systems. It indicates the adsorption process, which is endothermic in nature or exothermic. The calculated value of ΔH°, ΔS°, and ΔG° for sorption of cadmium onto *Leucaena leucocephala* activated carbon is listed in Table 6.

The negative values for the Gibbs free energy change, ΔG, indicate that the adsorption process for the cadmium was feasible and spontaneous. The increasing in ΔG values with increase in temperature showed the favorable adsorption was at higher temperatures. The result revealed the ΔH^o values obtained for the adsorption of cadmium onto *Leucaena leucocephala* activated carbon is positive for the C1-700. C2-700 and C3-700 show the negative values of ΔH^o. The positive value of ΔH^o indicates the endothermic nature of adsorbent, whereas the negative value of ΔH^o reflects the exothermic nature of the adsorbent interactions. The adsorptions of cadmium ions on all of the produced adsorbents are endothermic. This result was consistent for activated carbon made using an activation temperature of 750 °C and 800 °C. A rise in temperature would increase the rate of diffusion of the cadmium ions across the external boundary layer into the pores of the adsorbent particle, due to the decrement of the viscosity of the solution. Other possibilities are the amplification of pore size distribution and increment of the active surface sites with the increase in temperature. Most of the samples showed positive values of ΔS, showing the increment of an orderliness between the adsorbate and the adsorbent molecules (Koyuncu and Kul 2019).

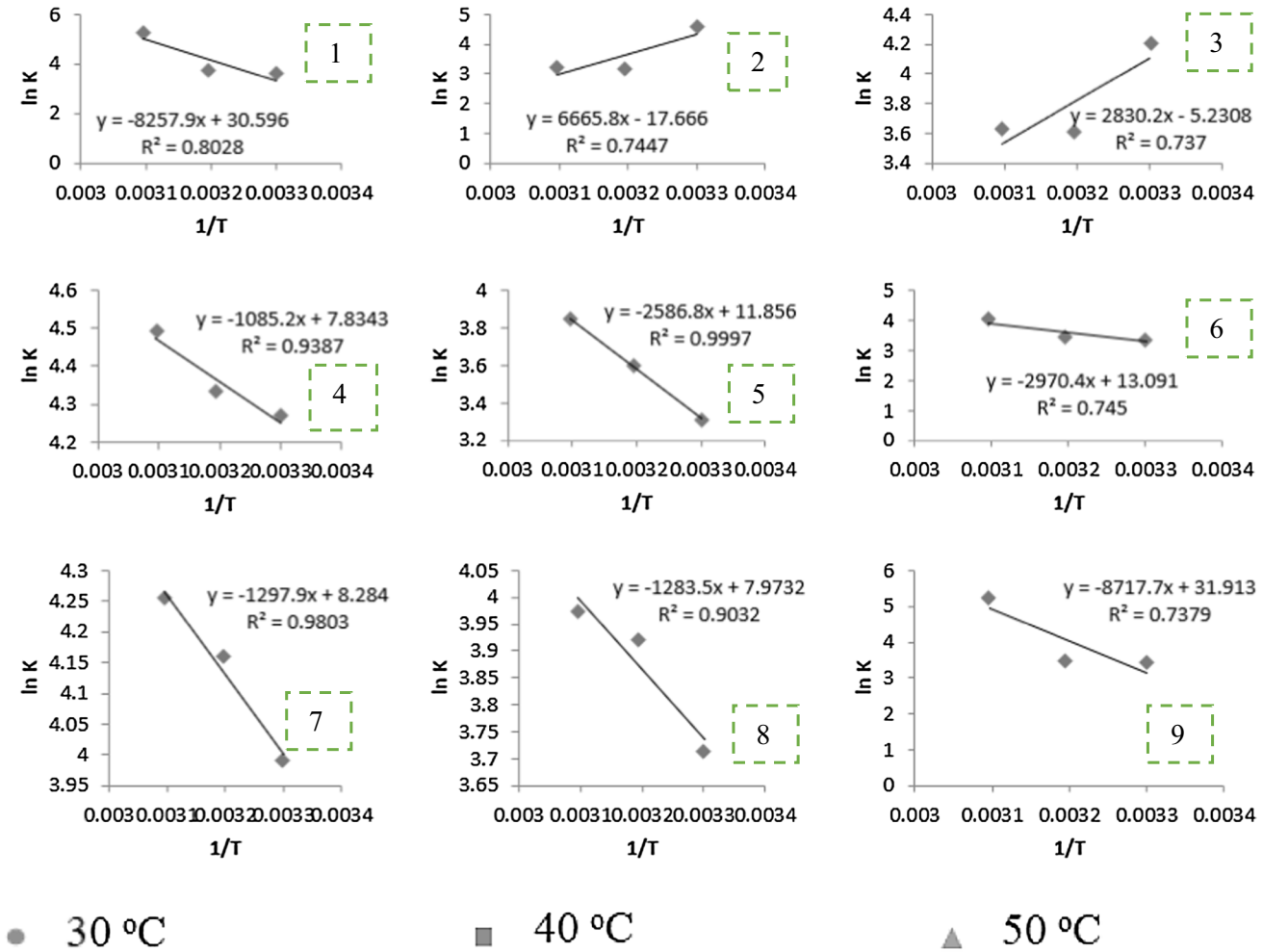

Fig. 7 Thermodynamic graph for samples C1-700 (1), C2-700 (2), C3-700 (3), C1-750 (4), C2-750 (5), C3-750 (6), C1-800 (7), C2-800 (8), and C3-800 (9)

Table 5 Langmuir and Freundlich isotherm models for the adsorption of cadmium at all activation temperatures

Sample	Temperature, °C	Langmuir Isotherm			Freundlich Isotherm		
		The maximum monolayer adsorption capacity	Langmuir constant	Correlation Coefficient	Affinity factor	Freundlich exponent	Correlation Coefficient
		q_{max} (mg/g)	K_L (l/mg)	R^2	K_F	l/n	R^2
C1-700	30	35.714	2.029	0.9925	3.6621	1.3812	0.8700
	40	41.667	1.086	0.9506	3.3951	1.3320	0.8662
	50	196.078	0.227	0.9728	4.0562	2.1336	0.9454
C2-700	30	95.238	1.280	0.9933	4.9962	2.2217	0.9672
	40	23.810	2.877	0.9879	3.3954	1.3890	0.9893
	50	24.752	4.440	0.9686	3.5172	1.1202	0.8870
C3-700	30	67.114	3.239	0.9700	4.6100	1.4739	0.7956
	40	37.037	1.317	0.9325	3.3128	1.1640	0.8222
	50	37.879	3.667	0.9776	4.0386	1.3659	0.9082
C1-750	30	71.429	1.261	0.9702	4.1160	1.5144	0.8520
	40	76.293	0.684	0.9804	3.9681	1.9205	0.9435
	50	89.256	0.982	0.9588	4.3979	1.8936	0.9285
C2-750	30	27.548	9.804	0.9850	4.7149	1.6614	0.9944
	40	36.496	3.262	0.9813	4.3202	1.7862	0.9599
	50	46.729	3.397	0.9752	4.6583	1.8036	0.9287
C3-750	30	29.586	12.071	0.9884	4.4273	1.3186	0.9521
	40	29.851	0.893	0.9774	2.9684	1.4263	0.9548
	50	54.645	0.436	0.9892	3.2605	2.0352	0.9804
C1-800	30	54.054	3.627	0.9627	4.8448	1.7987	0.9401
	40	64.013	2.600	0.9609	4.2177	1.2863	0.7513
	50	70.423	3.302	0.9873	5.7397	2.3551	0.9701
C2-800	30	40.984	8.133	0.9855	5.6249	2.1227	0.9703
	40	50.505	4.500	0.9783	4.7040	1.5924	0.9000
	50	53.191	5.371	0.9707	4.8970	1.6174	0.8874
C3-800	30	31.153	8.231	0.9671	3.8763	0.9878	0.8265
	40	31.447	5.483	0.9655	3.8045	1.0455	0.7990
	50	188.67	0.589	0.9542	5.1123	2.3296	0.9003

Conclusion

The *Leucaena leucocephala* biomass had been converted into activated carbon by chemical mean. Analysis of BET found out that higher surface area can be obtained using the higher activation temperature. Another finding from this work suggests that higher NaOH to carbonized sample ratios will create a larger surface area for all activation temperatures, which are 662 m^2g^{-1} for 700 °C activation temperature, 735 m^2g^{-1} for 750 °C, and 776 m^2g^{-1} for 800 °C. The FT-IR analysis detected a lesser number of functional groups in the activated carbon compared to raw *Leucaena leucocephala* due to deterioration effect of the heating process. The thermogravimetry analysis results concluded that even though the activated carbon made using higher NaOH: biomass ratio has the highest surface area, they are a little less thermally stable compared to the lower ratios at all activation temperatures. The activated carbon that is produced from *Leucaena leucocephala* biomass is fit to the Langmuir isotherm, regardless of any activation temperature, showing that the activated carbon produced is doing monolayer cadmium adsorption onto the surface. Also, the thermodynamic study revealed that the adsorption process is endothermic, reflected by the positive value of ΔH^o.

Table 6 Thermodynamic parameters of cadmium adsorption for all samples

Sample (°C)	Temperature (K)	ΔG^o (kJ/mole)	ΔH^o (kJ/mole)	ΔS^o (kJ/mol/K)
C1-700	303	−9.007	68.656	0.2544
	313	−9.706		
	323	−14.175		
C2-700	303	−11.478	−55.419	−0.1468
	313	−8.249		
	323	−8.617		
C3-700	303	−10.597	−23.530	−0.0434
	313	−9.399		
	323	−9.759		
C1-750	303	−10.754	15.674	0.0651
	313	−11.279		
	323	−12.062		
C2-750	303	−8.353	21.507	0.0986
	313	−9.361		
	323	−10.324		
C3-750	303	−8.533	24.696	0.1088
	313	−8.838		
	323	−10.744		
C1-800	303	−10.051	10.791	0.0689
	313	−10.823		
	323	−11.425		
C2-800	303	−9.354	10.671	0.0662
	313	−10.206		
	323	−10.672		
C3-800	303	−8.663	72.479	0.2653
	313	−8.973		
	323	−14.072		

Acknowledgement The authors acknowledged the Ministry of Education, Malaysia, for MyMaster scholarship to Wan Muhammad Hilmi bin Wan Ibrahim and Universiti Malaysia Kelantan for Short Term Grant (R/SGJP/A08.00/01046A/001/2015/000242) awarded to Mohd Hazim Mohamad Amini.

Financial Disclosure statement The author(s) received no specific funding for this work

Compliance with ethical standards

Conflict of interest The authors declared no conflict of interest and are mutually agreed on the publication of this work.

References

Adinata D, Wan Daud WMA, Aroua MK (2007) Preparation and characterization of activated carbon from palm shell by chemical activation with K2CO3. Bioresour Technol 98:145–149. https://doi.org/10.1016/j.biortech.2005.11.006

Alimsyah A, Damayanti A (2013) Penggunaan Arang Tempurung Kelapa dan Eceng Gondok untuk Pengolahan Air Limbah Tahu dengan Variasi Konsentrasi. Jurnal Teknik ITS 2:D6–D9

Amini MHM, Hashim R, Sulaiman NS, Sulaiman O, Lazim AM (2019) Environmentally Friendly Wood Composite Fabricated From Rubberwood Using Citric Acid Esterified Oil Palm Starch. Cellul Chem Technol 53:551–559

Bansal RC, Goyal M (2005) Activated carbon adsorption. CRC Press, Boca Raton

Cazetta AL et al (2011) NaOH-activated carbon of high surface area produced from coconut shell: Kinetics and equilibrium studies from the methylene blue adsorption. Chem Eng J 174:117–125. https://doi.org/10.1016/j.cej.2011.08.058

Chunhabundit R (2016) Cadmium exposure and potential health risk from foods in contaminated area. Thail Toxic Res 32:65–72. https://doi.org/10.5487/TR.2016.32.1.065

Danish M, Ahmad T (2018) A review on utilization of wood biomass as a sustainable precursor for activated carbon production and application. Renew Sustain Energy Rev 87:1–21. https://doi.org/10.1016/j.rser.2018.02.003

Gerçel Ö, Özcan A, Özcan AS, Gercel HF (2007) Preparation of activated carbon from a renewable bio-plant of Euphorbia rigida by H 2 SO 4 activation and its adsorption behavior in aqueous solutions. Appl Surf Sci 253:4843–4852

Gierszal KP, Yoon SB, Yu J-S, Jaroniec M (2006) Adsorption and structural properties of mesoporous carbons obtained from mesophase pitch and phenol-formaldehyde carbon precursors using porous templates prepared from colloidal silica. J Mater Chem 16:2819–2823

Gupta A, Meyer JM, Goel R (2002) Development of Heavy Metal-Resistant Mutants of Phosphate Solubilizing Pseudomonas sp. NBRI 4014 and Their Characterization. Curr Microbiol 45:323–327. https://doi.org/10.1007/s00284-002-3762-1

Hou C-H, Liu N-L, Hsi H-C (2015) Highly porous activated carbons from resource-recovered Leucaena leucocephala wood as capacitive deionization electrodes. Chemosphere 141:71–79. https://doi.org/10.1016/j.chemosphere.2015.06.055

Kim CH, Lee D-K, Pinnavaia TJ (2004) Graphitic mesostructured carbon prepared from aromatic precursors. Langmuir 20:5157–5159

Kim T-W, Ryoo R, Gierszal KP, Jaroniec M, Solovyov LA, Sakamoto Y, Terasaki O (2005) Characterization of mesoporous carbons synthesized with SBA-16 silica template. J Mater Chem 15:1560–1571

Koyuncu H, Kul AR (2019) Removal of aniline from aqueous solution by activated kaolinite: Kinetic, equilibrium and thermodynamic studies. Collid Surf A: Physicochem Eng Asp 569:59–66. https://doi.org/10.1016/j.colsurfa.2019.02.057

Kurniawan D (2004) Pengamatan Pengaruh Peringkat Batubara terhadap Daya Serap (iodine) Karbon Aktif. Skripsi Universitas Islam Bandung (UNISBA), Bandung h:1–20

Le Van K, Luong Thi TT (2014) Activated carbon derived from rice husk by NaOH activation and its application in supercapacitor.

Prog Nat Sci: Mater Int 24:191–198. https://doi.org/10.1016/j.pnsc.2014.05.012
Lee J, Kim J, Hyeon T (2006) Recent progress in the synthesis of porous carbon materials. Adv Mater 18:2073–2094
Lee YC, Amini MHM, Sulaiman NS, Mazlan M, Boon JG (2018) Batch adsorption and isothermic studies of malachite green dye adsorption using Leucaena leucocephala biomass as potential adsorbent in water treatment Songklanakarin. J Sci Technol 40:563–569
Li Z, Jaroniec M (2001) Colloidal imprinting: a novel approach to the synthesis of mesoporous carbons. J Am Chem Soc 123:9208–9209
Li Z, Wang G, Zhai K, He C, Li Q, Guo P (2018) Methylene blue adsorption from aqueous solution by loofah sponge-based porous carbons. Colloid Surf A 538:28–35. https://doi.org/10.1016/j.colsurfa.2017.10.046
Li Z, Sellaoui L, Luiz Dotto G, Bonilla-Petriciolet A, Ben Lamine A (2019) Understanding the adsorption mechanism of phenol and 2-nitrophenol on a biopolymer-based biochar in single and binary systems via advanced modeling analysis. Chem Eng J 371:1–6. https://doi.org/10.1016/j.cej.2019.04.035
Li Z et al (2019) Interpretation of the adsorption mechanism of Reactive Black 5 and Ponceau 4R dyes on chitosan/polyamide nanofibers via advanced statistical physics model. J Mol Liq 285:165–170. https://doi.org/10.1016/j.molliq.2019.04.091
Li Z et al (2020a) Adsorption of hazardous dyes on functionalized multiwalled carbon nanotubes in single and binary systems: experimental study and physicochemical interpretation of the adsorption mechanism. Chem Eng J 389:124467. https://doi.org/10.1016/j.cej.2020.124467
Li Z et al (2020b) Adsorption of congo red and methylene blue dyes on an ashitaba waste and a walnut shell-based activated carbon from aqueous solutions: Experiments, characterization and physical interpretations. Chem Eng J 388:124263. https://doi.org/10.1016/j.cej.2020.124263
Liu Q-S, Zheng T, Wang P, Guo L (2010) Preparation and characterization of activated carbon from bamboo by microwave-induced phosphoric acid activation. Ind Crops Prod 31:233–238
Loaiza JM, López F, García MT, García JC, Díaz MJ (2017) Biomass valorization by using a sequence of acid hydrolysis and pyrolysis processes. Appl to Leucaena leucocephala Fuel 203:393–402. https://doi.org/10.1016/j.fuel.2017.04.135
Meng Y et al (2005) Ordered mesoporous polymers and homologous carbon frameworks: amphiphilic surfactant templating and direct transformation. Angew Chem 117:7215–7221
Ningrum LP, Lusiana RA, Nuryanto R (2008) Dekolorisasi Remazol Brilliant Blue dengan Menggunakan Karbon Aktif Makalah Penelitian
Rafatullah M, Sulaiman O, Hashim R, Amini M (2011) Adsorption of Copper (II) Ions onto Surfactant-Modified Oil Palm Leaf Powder. J Dispers Sci Technol 32:1641–1648
Ryoo R, Joo SH, Kruk M, Jaroniec M (2001) Ordered mesoporous carbons. Adv Mater 13(9):677–681
Shi Q et al (2010) Preparation of activated carbon from cattail and its application for dyes removal. J Environ Sci 22:91–97
Singh A, Kumar D, Gaur JP (2007) Copper(II) and lead(II) sorption from aqueous solution by non-living Spirogyra neglecta. Bioresour Technol 98:3622–3629. https://doi.org/10.1016/j.biortech.2006.11.041
Smíšek M, Černý S (1970) Active carbon: manufacture, properties and applications vol 12. Elsevier Publishing Company, Amsterdam
Subadra I, Setiaji B, Tahir I Activated carbon production from coconut shell with (NH4) HCO3 activator as an adsorbent in virgin coconut oil purification. In: Prosiding Seminar Nasional DIES ke, 2005. pp 1–8
Sulaiman O, Amini MHM, Rafatullah M, Hashim R, Ahmad A (2010) Adsorption equilibrium and thermodynamic studies of copper (II) ions from aqueous solutions by oil palm leaves International Journal of Chemical Reactor Engineering 8
Sulaiman NS, Hashim R, Mohamad Amini MH, Danish M, Sulaiman O (2018) Optimization of activated carbon preparation from cassava stem using response surface methodology on surface area and yield. J Clean Prod 198:1422–1430. https://doi.org/10.1016/j.jclepro.2018.07.061
Tran HN, You S-J, Chao H-P (2017) Fast and efficient adsorption of methylene green 5 on activated carbon prepared from new chemical activation method. J Environ Manage 188:322–336. https://doi.org/10.1016/j.jenvman.2016.12.003
Uetani M, Kobayashi E, Suwazono Y, Kido T, Nogawa K (2006) Cadmium exposure aggravates mortality more in women than in men. Inte J Environ Health Res 16:273–279. https://doi.org/10.1080/09603120600734220
Wan Ibrahim WMH, Mohamad Amini MH, Sulaiman NS, Kadir WRA (2019) Powdered activated carbon prepared from Leucaena leucocephala biomass for cadmium removal in water purification process Arab. J Basic Appl Sci 26:30–40. https://doi.org/10.1080/25765299.2018.1533203
Wang X, Bozhilov KN, Feng P (2006) Facile preparation of hierarchically porous carbon monoliths with well-ordered mesostructures. Chem mater 18:6373–6381
Wong S, Ngadi N, Inuwa IM, Hassan O (2018) Recent advances in applications of activated carbon from biowaste for wastewater treatment: a short review. J Clean Prod 175:361–375. https://doi.org/10.1016/j.jclepro.2017.12.059
Wu H, Liao Q, Chillrud SN, Yang Q, Huang L, Bi J, Yan B (2016) Environmental exposure to cadmium: health risk assessment and its associations with hypertension and impaired kidney function. Sci Rep 6:29989
Yang J, Qiu K (2010) Preparation of activated carbons from walnut shells via vacuum chemical activation and their application for methylene blue removal. Chem Eng J 165:209–217. https://doi.org/10.1016/j.cej.2010.09.019
Yang H et al (2004) A simple melt impregnation method to synthesize ordered mesoporous carbon and carbon nanofiber bundles with graphitized structure from pitches. J Phys Chem B 108:17320–17328